

MATHEMATICAL MODELS OF COLORECTAL TUMOUR MICROSTRUCTURE INFORMED BY OSCILLATING GRADIENTS DIFFUSION MRI

Alessandro Proverbio¹, Bernard M. Sio^{2,3}, Eleftheria Panagiotaki³, Samuel Walker-Samuel², Mark F. Lythgoe², Adam P. Gibson¹, and Daniel C. Alexander³
¹Medical Physics and Bioengineering, University College London, London, United Kingdom, ²Centre for Advanced Biomedical Imaging, Division of Medicine, University College London, London, United Kingdom, ³Centre for Medical Image Computing and Department of Computer Science, University College London, London, United Kingdom

Target audience Biophysical modellers, cancer, diffusion MRI and microstructure imaging researchers.

Overview Investigation of tissue microstructure with non-invasive histology is a developing research area. Diffusion MRI (dMRI) can estimate features of microstructural components such as cell cytoarchitecture. Diffusion properties have been used to describe the response of tumours to treatment¹, for example, the apparent diffusion coefficient (ADC) provides contrast based on non-specific microstructural properties. Model based approaches^{2,3} potentially provide more specific information. For example² recently estimated microstructural features of two tumor types and showed their sensitivity to the response to treatment. Here we implement oscillating gradient dMRI to probe smaller components than cells such as nuclei, and compare various simple models relating the diffusion signal to features of the tumour microenvironment.

Purpose We develop signal models for oscillating gradient dMRI and various tissue models that consist of different combinations of components, with the aim of increasing the sensitivity to small cellular components over Pulse Gradient Spin Echo (PGSE). Experiments characterize the relationship between signal and oscillation frequency and identify the model that best describes the signal. Finally, we aim to report the specificity of the estimates from the best model on the signals from two colorectal tumours xenograft models, which display different levels of differentiation.

Methods This study is performed *ex-vivo* on 6 subcutaneous xenograft tumour samples grown in nude mice: 3 LS174T (LS), and 3 SW1222 (SW) cell lines. They were left to grow for 3 weeks then fixed in paraformaldehyde (PFA). Tumours were preserved for 1 year and subsequently scanned with a 9.4T Agilent VNMRS scanner.

Diffusion MRI measurements were acquired with Square Wave Oscillating Gradient Spin Echo (SWOGSE)⁴. Sequences were acquired for gradient $G = 0, 0.05, 0.1, 0.15, 0.2, 0.3, 0.4, 0.5, 0.7 \text{ T/m}$, and for frequency $f = 50, 100, 150, 250 \text{ Hz}$, diffusion time, $\Delta = 26\text{ms}$, gradient duration, $\delta = 21\text{ms}$, minimum echo time, and $\text{TR} = 4\text{s}$. Imaging parameters were: 64×64 matrix, 6 slices, $0.25 \times 0.25 \times 1 \text{ mm}^3$ resolution, four shots EPI readout. ROIs were selected by manually segmenting the tissue and by applying a mask to exclude susceptibility artefacts.

The signal is processed using 8 microstructural models (combination of compartments shown in figure 1)^{3,5}. Non microstructurally specific models MonoExp, BiExp and TriExp combine one, two and three Ball compartments. The other models all represent restriction within cells and nuclei with combinations of spherical and spherical shell restricting compartments. The lognDSph and normDSph model a distribution of spheres with logNormal and Gaussian distribution of radii. The models She+Sph and Sph+Sph represent the cells and their nuclei. We used a Monte Carlo Markov Chain (MCMC) algorithm to compare the specificity of the estimates.

Histology investigation was performed on a representative set of samples surgically resected and fixed in PFA. They were sectioned at $10 \mu\text{m}$, stained for morphology with haematoxylin and eosin, and viewed at $\times 40$ magnification with a Axioskop 2 microscope (Carl Zeiss, UK).

Results Figure 2 shows the variation of Mean Diffusivity (MD) with the frequency of oscillation of the gradient. There was no statistically significant difference in MD, between tumour types, but a constant increase of MD with the frequency suggests the sensitivity of different frequencies to different length scales. A shorter gradient oscillation period reduces the effective diffusion time of the spins.

Table 1 shows a ranking of models based on Bayesian Information Criterion (BIC). Anisotropic models were excluded since the Fractional Anisotropy obtained with a DTI dataset is below 0.3 in the datasets. The models composed of confined compartments are the best ranked. She+Sph+Ball is the best in both the cell lines, but similar BIC is obtained with DSph models where the presence of multiple Sph compartments spanning a defined set of radii distribution appears to improve signal fitting.

Figure 3 shows three of the estimates from the best performing model. The sizes of the cellular compartment, R , are underestimated (histology: SW = $8.0 \pm 0.4 \mu\text{m}$; LS = $11.2 \pm 2 \mu\text{m}$) as well as the volume fractions Vf (histology: SW = 0.80 ± 0.02 ; LS = 0.79 ± 0.01). The maximum width of the MCMC chain is in the same order of the histology uncertainty of the dimensional estimates. Histology for the inner compartment is not available but the accuracy of the estimates for r is often limited by the constraints on the diffusivity fitting.

Discussion and conclusion Oscillating Gradient Spin Echo probes shorter length scales than standard PGSE potentially providing additional information about the tissue microstructure. The more tissue-like compartment model appears to represent the signal better, suggesting the feasibility of a clinical measurement of cytological properties of the tissue. The best models appear to be very specific in the identification of cell size, but instabilities occur in the estimation of nuclei size. This is possibly due to the presence of multiple nuclei or the small length scales observed. *In-vivo* measurements could provide a novel approach to lesion staging.

References 1. D.C. Colvin, et al., Magnetic Resonance Imaging 29 (2011); 2. E. Panagiotaki, et al., Proc. Int. Soc. Mag. Reson. Med. 21 (2013); 3. E. Panagiotaki, et al., NeuroImage 59 (2012); 4. A. Ianus, et al., Journal of Magnetic Resonance 200 (2012); 5. J. Xu, et al., Journal of Magnetic Resonance 200 (2009)

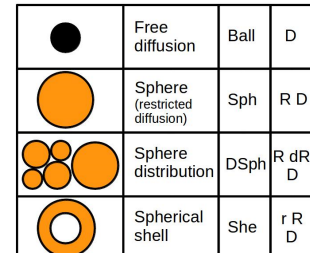


Figure 1: Scheme of the models of diffusion.

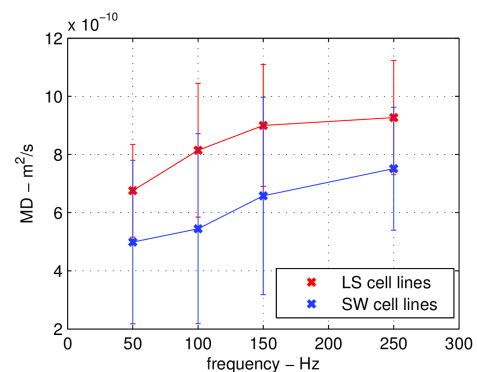


Figure 2: Variation of diffusivity with the gradient oscillation frequency. The error bars show the SD between samples.

Rank (BIC)	BIC	LS	# par	BIC	SW	# par
1	-160.2	She+Sph+Ball	6	-162.0	She+Sph+Ball	6
2	-158.8	Sph+Sph+Ball	6	-161.5	Sph+Sph+Ball	6
3	-158.2	normDSph+Ball	5	-159.1	lognDSph+Ball	5
4	-156.8	lognDSph+Ball	5	-155.4	normDSph+Ball	5
5	-151.3	Ball+Sph	4	-146.0	Ball+Sph	4
6	-133.6	BiExp	3	-132.1	BiExp	3
7	-130.2	TriExp	5	-127.0	TriExp	5
8	-97.2	MonoExp	1	-101.8	MonoExp	1

Table 1: Model ranking based on BIC

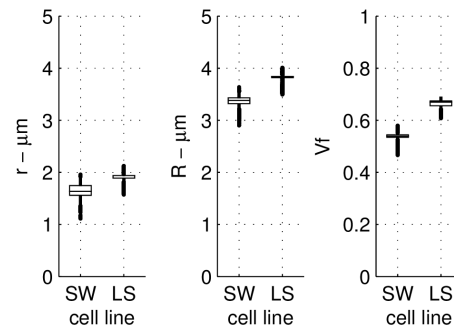


Figure 3: MCMC for the nuclear size, r , the cell size, R , and the volume fraction, Vf . Boxplots from one LS and one SW sample, show median and first and fourth quartile and the outliers.